SLAC-PUB-12344

CHARM AND CHARMONIUM SPECTROSCOPY FROM B-FACTORIES

ANTIMO PALANO

INFN and Dipartimento di Fisica, University of Bari
Via Orabona 4, Bari, 70126, Italy
antimo@ba.infn.it

For BaBar Collaboration

New and recent results are presented on charm and charmonium spectroscopy from BABAR experiment at SLAC. In particular, measurements on D_{sJ} states branching fractions have been performed both in B-decays and inclusive $e^+e^- \to c\bar{c}$ interactions. Here a search for $D_{sj}(2632)$ has been performed and a new D_{sJ} state at a mass of 2.856 GeV/c^2 has been observed. A search for $Y(4260)$ has been performed in exclusive $D\bar{D}$ production from initial-state radiation.

Keywords: charm; charmonium.

PACS numbers: 11.40.Lb, 13.25.Ft, 13.20.Fc

1. New Measurements of D_{sJ} properties.

The recently discovered $D^*_{sJ}(2317)^+$ and and $D_{sJ}(2460)^+$ mesons, does not conform to conventional models of $c\bar{s}$ meson spectroscopy. The possibility that these are exotic states has attracted considerable experimental and theoretical interest and has focused renewed attention on the subject of charmed-meson spectroscopy in general.

An updated analysis of these two states using 232 fb^{-1} of $e^+e^- \to c\bar{c}$ has been performed [1]. Shown in Fig. 1(left) is the invariant mass distribution of the $D^+_s\pi^0$ combinations. Signals from $D^*_s(2112)^+$ and $D^*_{sJ}(2317)^+$ decay are evident. An unbinned likelihood fit is applied to this mass distribution in order to extract the parameters and yield of the $D^*_{sJ}(2317)^+$ signal and upper limits on $D_{sJ}(2460)^+$ decay. The resulting $D^*_{sJ}(2317)^+$ mass is shown in table 1.

The $D^+_s\gamma$ mass distribution is shown in Fig. 1(right). Clear evidence for $D_{sJ}(2460)^+$ can be seen together with the reflection of $D^*_{sJ}(2317)^+ \to D^+_s\pi^0$ with a missing γ. The $D^+_s\pi^0\gamma$ mass distribution in the $D^*_s(2112)^+$ signal region and sidebands are shown in Fig. 2(left). A clear $D_{sJ}(2460)^+$ signal can be seen, together with reflections from $D^*_{sJ}(2317)^+$ and $D^*_s(2112)^+$. The invariant mass distribution of the $D^+_s\pi^+\pi^-$ candidates is shown in Fig. 2(right) where clear peaks from $D_{sJ}(2460)^+$ and $D_{s1}(2536)^+$ decay are apparent.

Contributed to International Workshop on Tau-Charm Physics (Charm 2006), 5-7 June 2006, Beijing, China

Work supported in part by the US Department of Energy contract DE-AC02-76SF00515

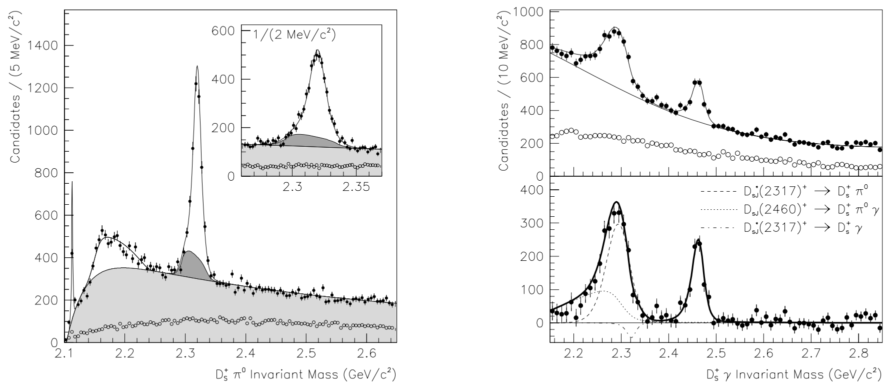

Fig. 1. Left. The invariant mass distribution for (solid points) $D_s^+\pi^0$ candidates and (open points) the equivalent using the D_s^+ sidebands. Included in this fit is (light shade) a contribution from combinatorial background and (dark shade) the reflection from $D_{sJ}(2460)^+ \rightarrow D_s^*(2112)^+\pi^0$ decay. Right. The $D_s^+\gamma$ invariant mass distribution. The solid points in the top plot are the mass distribution. The open points are the D_s^+ sidebands, scaled appropriately. The bottom plot shows the same data after subtracting the background curve from the fit. Various contributions to the likelihood fit are also shown.

Table 1. A summary of the combined mass and width results. The first quoted uncertainty is statistical and the second is systematic.

Particle	Mass (MeV/c^2)	Γ (MeV)
$D_{sJ}^*(2317)^+$	2319.6 $\pm$ 0.2 $\pm$ 1.4	< 3.8
$D_{sJ}(2460)^+$	2460.1 $\pm$ 0.2 $\pm$ 0.8	< 3.5
$D_{s1}(2536)^+$	2534.6 $\pm$ 0.3 $\pm$ 0.7	< 2.5

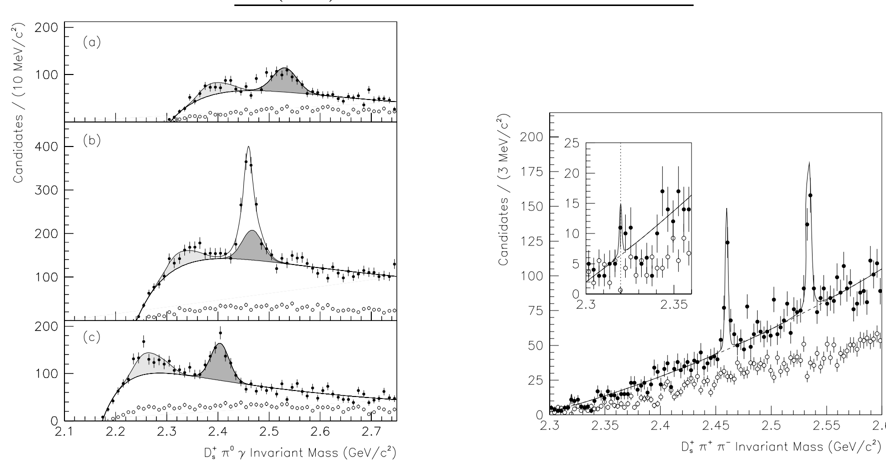

Fig. 2. Left. The invariant mass distribution of $D_s^+\pi^0\gamma$ candidates in the (a) upper, (b) signal, and (c) lower in the $D_s^+\gamma$ mass selection windows close to $D_s^*(2112)^+$ for (solid points) the D_s^+ signal and (open points) D_s^+ sideband samples. The dark gray (light gray) region corresponds to the predicted contribution from the $D_{sJ}^*(2317)^+$ ($D_s^*(2112)^+$) reflection. Right. The invariant mass distribution of (solid points) $D_s^+\pi^+\pi^-$ candidates and (open points) the equivalent using the D_s^+ sidebands. The dotted line in the insert indicates the $D_{sJ}^*(2317)^+$ mass.

The mass and width results for the $D_{sJ}^*(2317)^+$, $D_{sJ}(2460)^+$, and $D_{s1}(2536)^+$ mesons are summarized in Table 1. The $D_{sJ}(2460)^+$ mass is the average of that obtained from the $D_s^+\gamma$, $D_s^+\pi^0\gamma$, and $D_s^+\pi^+\pi^-$ final states, although the latter measurement dominates in the average due to superior systematic uncertainties.

A search has been performed for $D_{sJ}(2317)$ decays to $D_s^+\pi^-$ and $D_s^+\pi^+$ finding no signal. A summary of the branching-ratio and limits is displayed in table 2.

2. Measurement of D_s^- and $D_{sJ}(2460)^-$ Branching Fractions.

This analysis uses $\Upsilon(4S) \to B\overline{B}$ events in which either a B^+ or a B^0 meson decays into a fully reconstructed hadronic final state [2]. The recoiling B meson, on the other hand, decays to two charm mesons, i.e. $\overline{B} \to D_{\rm meas}D_X$. Here $D_{\rm meas}$ represents a fully reconstructed $D^{(*)+,0}$ or $D_s^{(*)-}$ meson, and the mass and momentum of the D_X are inferred from the kinematics of the two-body B decay. This study allows measurements of B branching fractions without any assumption on the decays of the D_X. The measurements are based on an integrated luminosity of 210.5 fb^{-1} From two separate classes of events with $D_{\rm meas} = D_s^{(*)-}$ and with $D_X = D_s^{(*)-}$ we measure the branching fraction of $D_s^- \to \phi\pi^-$, which has important implications for a wide range of D_s and B physics. Furthermore, we select final states with $D_X = D_{sJ}(2460)^-$ and combine with the *BABAR*

Table 2. A summary of branching-ratio results. The first quoted uncertainty for the central value is statistical and the second is systematic. The limits correspond to 95% CL.

Decay Mode	Central Value	Limit
$\mathcal{B}(D_{sJ}^*(2317)^+ \to X)/\mathcal{B}(D_{sJ}^*(2317)^+ \to D_s^+\pi^0)$		
$D_s^+\gamma$	$-0.02 \pm 0.02 \pm 0.08$	< 0.14
$D_s^+\pi^0\pi^0$	$0.08 \pm 0.06 \pm 0.04$	< 0.25
$D_s^+\gamma\gamma$	$0.06 \pm 0.04 \pm 0.02$	< 0.18
$D_s^*(2112)^+\gamma$	$0.00 \pm 0.03 \pm 0.07$	< 0.16
$D_s^+\pi^+\pi^-$	$0.0023 \pm 0.0013 \pm 0.0002$	< 0.0050
$\mathcal{B}(D_{sJ}(2460)^+ \to X)/\mathcal{B}(D_{sJ}(2460)^+ \to D_s^+\pi^0\gamma)$ [a]		
$D_s^+\pi^0$	$-0.023 \pm 0.032 \pm 0.005$	< 0.042
$D_s^+\gamma$	$0.337 \pm 0.036 \pm 0.038$	—
$D_s^*(2112)^+\pi^0$	$0.97 \pm 0.09 \pm 0.05$	> 0.75
$D_{sJ}^*(2317)^+\gamma$	$0.03 \pm 0.09 \pm 0.05$	< 0.25
$D_s^+\pi^0\pi^0$	$0.13 \pm 0.13 \pm 0.06$	< 0.68
$D_s^+\gamma\gamma$	$0.08 \pm 0.10 \pm 0.04$	< 0.33
$D_s^*(2112)^+\gamma$	$-0.02 \pm 0.08 \pm 0.10$	< 0.24
$D_s^+\pi^+\pi^-$	$0.077 \pm 0.013 \pm 0.008$	—
$\sigma(D_{sJ}^*(2317)^{++})/\sigma(D_{sJ}^*(2317)^+)\times$ $\mathcal{B}(D_{sJ}^*(2317)^{++} \to X)/\mathcal{B}(D_{sJ}^*(2317)^+ \to D_s^+\pi^0)$		
$D_s^+\pi^+$	—	< 0.017
$\sigma(D_{sJ}^*(2317)^0)/\sigma(D_{sJ}^*(2317)^+)\times$ $\mathcal{B}(D_{sJ}^*(2317)^0 \to X)/\mathcal{B}(D_{sJ}^*(2317)^+ \to D_s^+\pi^0)$		
$D_s^+\pi^-$	—	< 0.013

[a] Denominator includes both $D_s^*(2112)^+\pi^0$ and $D_{sJ}^*(2317)^+\gamma$ channels.

measurements of $\mathcal{B}(\overline{B} \to D^{(*)+,0} D_{sJ}(2460)^-) \times \mathcal{B}(D_{sJ}(2460)^- \to D_s^{*-}\pi^0)$ and $\mathcal{B}(B \to D^{(*)+,0} D_{sJ}(2460)^-) \times \mathcal{B}(D_{sJ}(2460)^- \to D_s^-\gamma)$ [3], thus extracting for the first time the absolute branching fractions of this recently observed state.

One example of distribution of m_X is shown in Fig. 3. We obtain the following branching fractions:

$$\mathcal{B}(D_{sJ}(2460)^- \to D_s^{*-}\pi^0) = (56 \pm 13_{\text{stat.}} \pm 9_{\text{syst.}})\%,$$
$$\mathcal{B}(D_{sJ}(2460)^- \to D_s^-\gamma) = (16 \pm 4_{\text{stat.}} \pm 3_{\text{syst.}})\%,$$
$$\mathcal{B}(D_s^- \to \phi\pi^-) = (4.62 \pm 0.36_{\text{stat.}} \pm 0.50_{\text{syst.}})\%.$$

Our results show that the $D_{sJ}(2460)^-$ meson decays via photon or π^0 emission to $D_s^{(*)-}$ in $(72 \pm 19)\%$ of the cases.

3. Search for $D_{sJ}(2632)$.

The SELEX Collaboration at FNAL has reported the existence of a narrow state at a mass of 2632 MeV/c^2 decaying to $D_s^+\eta$ [4]. That analysis was based on a sample of about 500 D_s^+ events. Evidence for the same state in the corresponding D^0K^+ mass spectrum was also presented. This work has generated considerable theoretical interest because of the anomalous decay mode and since the state appears to have a small width despite having a mass significantly above D^0K threshold.

In the present analysis, inclusive production of the $D_s^+\eta$, D^0K^+, and $D^{*+}K_S$ systems is investigated in a search for the $D_{sJ}^*(2632)^+$ state. The analysis makes use of an integrated luminosity of 125 fb^{-1} and a D_s^+ yield of approximately 196,000 events. For events containing a D_s^+ candidate, η candidates are selected in the $\gamma\gamma$ decay mode. The resulting η signal consists of approximately 3900 events. Fig. 4(left)

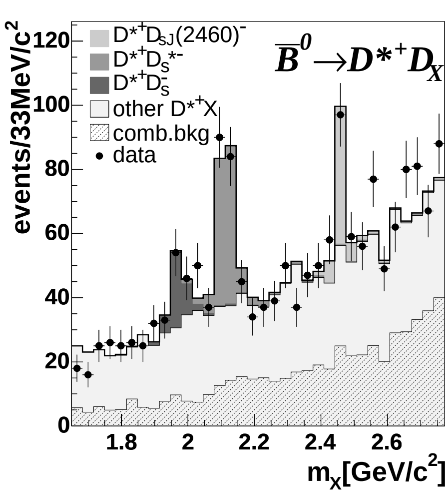

Fig. 3. One example of distribution of m_X for $\overline{B}^0 \to D^{*+}D_X$. Fitted $\overline{B}^0 \to D^{(*)+,0}D_s^{(*)-}$ and $\overline{B} \to D^{(*)+,0}D_{sJ}(2460)^-$ signal contributions and background components, are overlaid to the data points.

shows the scatterplot of $m(\gamma\gamma)$ versus $m(K^+K^-\pi^+)$ with the additional requirement that the e^+e^- center-of-mass momentum $p^*(D_s^+\eta)$ of the $D_s^+\eta$ system is at least 2.5 GeV/c to suppress background. The η and D_s^+ signal regions are quite clear. In order to establish the presence of an excess of events in the overlap region corresponding to correlated D_s^+ and η production, we perform a two-dimensional subtraction. The scatterplot is divided into the nine subregions of equal area. These subregions are centered on the D_s^+ and η mass values and extend by plus or minus 2.5 standard deviations in each mass variable.

The background subtracted $D_s^+\eta$ mass spectrum in the mass region below 3.0 GeV/c^2 is shown in Fig. 4(right). The arrow indicates the location at which the $D_{sJ}^*(2632)^+$ state should appear. There is no evidence for a signal.

We have also analyzed the D^0K^+ and $D^{*+}K_S$ mass spectra finding no evidence for structure in the 2.632 GeV/c^2 mass region.

4. Observation of a new D_{sJ} meson at a mass of 2.860 GeV/c^2.

We report here on a new $c\bar{s}$ state observed in the decay channels D^0K^+ and $D^+K_S^0$. This analysis is based on a 240 fb^{-1} data sample. We observe three inclusive processes:

$$e^+e^- \to D^0K^+X, D^0 \to K^-\pi^+ \tag{1}$$
$$e^+e^- \to D^0K^+X, D^0 \to K^-\pi^+\pi^0 \tag{2}$$
$$e^+e^- \to D^+K_S^0X, D^+ \to K^-\pi^+\pi^+, K_S^0 \to \pi^+\pi^- \tag{3}$$

Selecting events in the D signal regions, Fig. 5 shows the D^0K^+ invariant mass distributions for channels (1) and (2), and the $D^+K_S^0$ invariant mass distribution for channel (3). The three mass spectra in Fig. 5 present similar features. A single bin peak at 2.4 GeV/c^2 due to a reflection from the decays of $D_{s1}(2536)^+$ to $D^{*0}K^+$ or

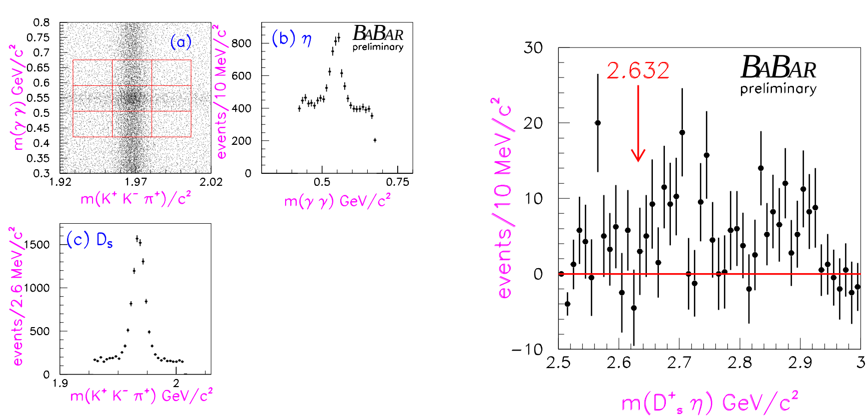

Fig. 4. Left. (a) The scatterplot of $m(\gamma\gamma)$ vs. $m(K^+K^-\pi^+)$ for $p^*(D_s^+\eta) > 2.5$ GeV/c. (b) The $\gamma\gamma$ and (c) $K^+K^-\pi^+$ mass projections for the selected region. Right. The $D_s^+\eta$ invariant mass distribution for the region below 3 GeV/c^2. The arrow indicates the mass location at which the $D_{sJ}^*(2632)^+$ state should appear.

$D^{*+}K^0_S$ in which the π^0 or γ from the D^* decay is missed. A broad structure peaking at a mass of approximately 2.7 GeV/c^2. An enhancement around 2.86 GeV/c^2. This can be seen better in the expanded views shown in the insets of Fig. 5.

Table 3 summarizes the χ^2 probabilities, the number of $D_{sJ}(2860)^+$ events (with statistical and systematic errors) and the $D_{sJ}(2860)^+$ statistical significances from the three separate fits to the DK mass spectra. Fig. 6 shows the background-subtracted $D^0_{K^-\pi^+}K^+$, $D^0_{K^-\pi^+\pi^0}K^+$, and $D^+_{K^-\pi^+\pi^+}K^0_s$ invariant mass distributions in the 2.86 GeV/c^2 mass region. Fig. 6(d) shows the sum of the three mass spectra. We obtain the mass and width of $D^*_{s2}(2573)^+$:

$$m(D^*_{s2}(2573)^+) = (2572.2 \pm 0.3 \pm 1.0),\ \Gamma(D^*_{s2}(2573)^+) = (27.1 \pm 0.6 \pm 5.6)\ \text{MeV}/c^2,$$

where the first errors are statistical and the second systematic. For the new state we find

$$m(D_{sJ}(2860)^+) = (2856.6 \pm 1.5 \pm 5.0),\ \Gamma(D_{sJ}(2860)^+) = (47 \pm 7 \pm 10)\ \text{MeV}/c^2.$$

The broad structure around 2.7 GeV/c^2 has been parametrized with a Gaussian. In a fit which assumes the $X(2690)^+$ as an additional resonance its parameters are

$$m(X(2690)^+) = (2688 \pm 4 \pm 3),\ \Gamma(X(2690)^+) = (112 \pm 7 \pm 36)\ \text{MeV}/c^2.$$

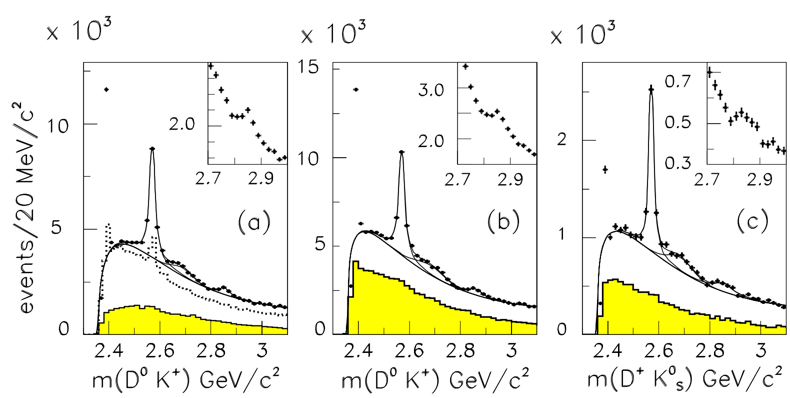

Fig. 5. The DK invariant mass distributions for (a) $D^0_{K^-\pi^+}K^+$, (b) $D^0_{K^-\pi^+\pi^0}K^+$ and (c) $D^+_{K^-\pi^+\pi^+}K^0_s$. The shaded histograms are for the D-mass sideband regions. The dotted histogram in (a) is from $e^+e^- \to c\bar{c}$ Monte Carlo simulations with an arbitrary normalization. The insets show an expanded view of the 2.86 GeV/c^2 region.

Table 3. χ^2 probabilities, $D_{sJ}(2860)^+$ event yields and statistical significances from the three separate fits to the DK mass spectra.

Channel	χ^2 probability (%)	$D_{sJ}(2860)^+$ events	Statistical significance
$D^0_{K^-\pi^+}K^+$	17	886 ± 134 ± 49	6.2 σ
$D^0_{K^-\pi^+\pi^0}K^+$	3	1146 ± 157 ± 78	6.5 σ
$D^+_{K^-\pi^+\pi^+}K^0_s$	21	371 ± 84 ± 53	3.7 σ

5. Study of the Exclusive Initial-State Radiation Production of the $D\bar{D}$ System.

The $Y(4260)$ structure was discovered in the initial-state radiation (ISR) process $e^+e^- \to \gamma_{ISR}\pi^+\pi^- J/\psi$ [5] at the energy where the total e^+e^- hadronic cross section shows a local minimum [6]. Its spin-parity assignment, $J^{PC} = 1^{--}$ is inferred because it can be produced by a single-photon annhilation mechanism. A study of exclusive production of the $D\bar{D}$ system through initial-state radiation is performed in a search for charmonium states using the following reactions:

$$e^+e^- \to \gamma_{ISR}\; D^0\overline{D}^0, D^0 \to K^-\pi^+, \overline{D}^0 \to K^+\pi^- \tag{4}$$
$$e^+e^- \to \gamma_{ISR}\; D^0\overline{D}^0, D^0 \to K^-\pi^+\pi^0, \overline{D}^0 \to K^+\pi^- \tag{5}$$
$$e^+e^- \to \gamma_{ISR}\; D^0\overline{D}^0, D^0 \to K^-\pi^+\pi^+\pi^-, \overline{D}^0 \to K^+\pi^- \tag{6}$$
$$e^+e^- \to \gamma_{ISR}\; D^+D^-, D^+ \to K^-\pi^+\pi^+, D^- \to K^+\pi^-\pi^-. \tag{7}$$

The analysis makes use of an integrated luminosity of 288.5 fb^{-1}. A distinguishing characteristic of $e^+e^- \to \gamma_{ISR}D\bar{D}$ events is that the squared invariant mass of the recoil to the $D\bar{D}$ system (MM^2) is that of the initial-state photon. The peak centered on MM^2= 0 in Fig. 7(left), summed over all four reconstructed channels, provides clear evidence for exclusive ISR production. The shaded histogram shows a background estimate derived from the two-dimensional D and $\bar{D}$ mass sidebands. Candidate events in the ISR region, defined as $|MM^2| < 1.0$ GeV$^2/c^4$ are retained.

The $D\bar{D}$ invariant mass spectrum for the ISR sample is shown by the data points in Fig. 7(right). A clear signal is seen for the $\psi(3770)$, which decays predominantly to $D\bar{D}$. Additional enhancements coincide with the $\psi(4040)$, $\psi(4160)$ and $\psi(4415)$ masses. Finally, a broad enhancement is evident near 3.9 GeV/c^2. This structure has not been seen in the hadronic cross section measurements but is in qualitative agreement with coupled-channel model predictions [7]. An unbinned maximum likelihood fit is performed using a signal shape described by four relativistic P-wave Breit-Wigner distributions convoluted with a P-wave phase space function. The Breit-Wigner parameters are fixed to the values from a fit to the hadronic cross section [8]. A Gaussian term is used to parameterize the enhancement near 3.9 GeV/c^2. All Breit-Wigner and Gaussian terms are allowed to interfere by assigning

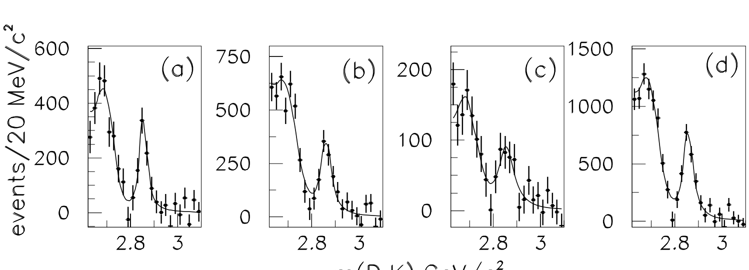

Fig. 6. Background-subtracted DK invariant mass distributions for (a) $D^0_{K^-\pi^+}K^+$, (b) $D^0_{K^-\pi^+\pi^0}K^+$, (c) $D^+_{K^-\pi^+\pi^+}K^0_s$, and (d) the sum of all modes in the 2.86 GeV/c^2 mass region.

them a free phase. A constant background is fixed to a value of 0.84 events per 20 MeV/c^2 bin as determined from a fit to the D and $\bar{D}$ mass sidebands. The fit yields a Gaussian-term mass of (3.909 ± 0.021) GeV/c^2 with $\sigma = (0.050 \pm 0.007)$ GeV/c^2. The $D\bar{D}$ mass resolution at the $Y(4260)$ mass, determined from Monte Carlo studies, is small compared to the widths of the fit structures and is neglected. No statistically significant signal for $Y(4260) \to D\bar{D}$ is established and we obtain an upper limit:

$$\frac{\mathcal{B}(Y(4260) \to D\bar{D})}{\mathcal{B}(Y(4260) \to J/\psi\pi^+\pi^-)} < 7.6 \text{ at } 95\% \text{ C.L.}$$

This limit is over an order of magnitude smaller than the value found for the $\psi(3770)$, another indication that the $Y(4260)$ may not be a conventional vector charmonium state.

References

1. *BABAR* Collab. (B. Aubert *et al.*), hep-ex/0604030, to appear in *Phys. Rev. D.*
2. *BABAR* Collab. (B. Aubert *et al.*), hep-ex/0605036, to appear in *Phys. Rev. D. (Rapid Communications)*
3. *BABAR* Collab. (B. Aubert *et al.*), *Phys. Rev. Lett.* **93**, 181801 (2004).
4. SELEX Collab. (A.V.Evdokimov *et al.*), *Phys. Rev. Lett.* **93**, 242001 (2004).
5. *BABAR* Collab., (B. Aubert *et al.*), *Phys. Rev. Lett.* **95**, 142001 (2005).
6. BES Collab. (J.Z. Bai *et al.*), *Phys. Rev. Lett.* **88**, 101802 (2002).
7. E. Eichten *et al.*, *Phys. Rev.* **D21**, 203 (1980).
8. K. Seth, hep-ex/0405007.

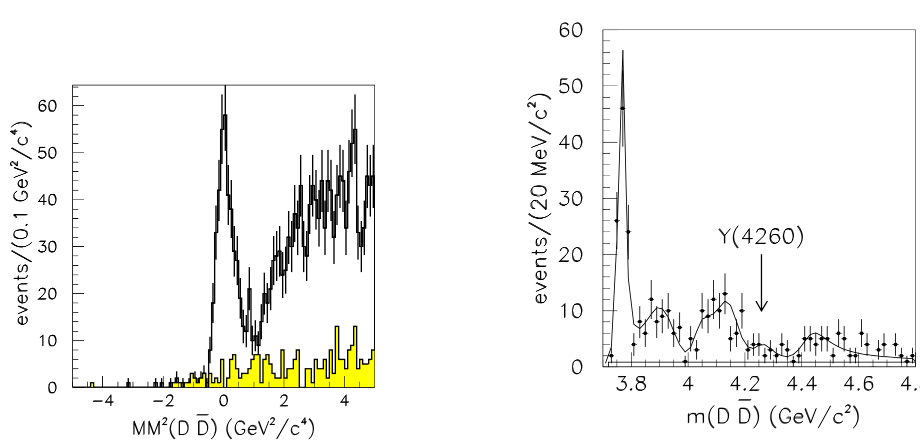

Fig. 7. Left. The recoil mass squared for ISR event candidates (MM^2) summed over a ll the four reconstructed final states. The shaded histogram is the background distribution estimated from D and $\bar{D}$ mass s idebands. Right. The $D\bar{D}$ invariant mass spectrum, with a fit that includes the $Y(4260)$ contribution. The arrow indicates the expected position of the $Y(4260)$.